铜钢堆焊接头的超声信号特征及质量评价

高双胜[1]， 刚 铁[1]， 桂光正[2]， 袁 媛[1]
（1. 哈尔滨工业大学 现代焊接生产技术国家重点实验室，哈尔滨 150001；
2. 宝山钢铁股份有限公司 宝钢分公司钢管厂，上海 201900）

高双胜

摘 要：采用水浸聚焦超声 C 扫描成像的检测方法，研究了铜钢堆焊接头的质量评价。首先从理论上分析了聚焦声束垂直于圆柱形工件表面入射时，沿圆柱体轴线与圆周两个互相垂直的方向上的声场情况。在此基础上对堆焊试件进行了超声 C 扫描检测试验，为了验证检测结果的可靠性，在试件上典型位置处进行了破坏性检测试验，分析了相应的超声 A 扫描信号特征。结果表明，采用该方法评定铜钢堆焊接头质量是可行的，同时指出采用从基体一侧入射的检测方式能够获得较高的可靠性。

关键词：异种材料连接；堆焊；超声 C 扫描；水浸聚焦
中图分类号：TG115.28 文献标识码：A 文章编号：0253－360X(2007)05－101－04

0 序 言

异种材料连接既实现了特殊的功用，又节约了制造成本，被广泛应用于工业生产的各个领域。异种材料连接技术主要有粘接、焊接及机械连接等。焊接作为一门综合性的材料加工技术，已成为异种材料连接的重要手段，常用的异种材料焊接方法有钎焊、堆焊、扩散焊等[1－3]。堆焊是目前应用比较广泛的一种焊接工艺，较多情况下用于异种材料连接。如在钢基体上堆焊不锈钢、耐热钢、铜合金等。铜钢连接属于传统的异种材料连接，随着工业生产的快速发展，铜钢连接结构在更多的领域得到了广泛的应用。近年来国内外在这方面做了大量的试验研究，取得了一些成果[4,5]。

现代工业生产对上述连接接头的质量提出了新的更高的要求，采用高效、可靠的无损检测方法对异种材料连接接头的质量做出客观的评价，是目前亟待解决的问题。超声波和 X 射线是现代无损检测技术中应用最为广泛的检测手段，受检测原理的限制，X 射线检测方法难以发现堆焊和扩散焊中的未熔合缺陷。超声成像无损检测方法因其设备简单、操作方便快捷，在科学研究及生产实践中应用广泛[6,7]。采用水浸聚焦超声 C 扫描成像的检测方法，研究了异种材料连接界面的超声信号特征，为接头质量评价和焊接工艺的改进提供有益的参考。

收稿日期：2006－06－05

1 试 验

1.1 试验材料

研究对象为大直径环形工件上的堆焊界面层，基体材料为合金结构钢，堆焊层为铜合金。异种材料连接常在界面处产生各种缺陷。根据此类连接结构特点，采用径向垂直入射水浸聚焦超声 C 扫描成像的方法进行检测。图 1 为堆焊结构检测示意图，试验中使用的探头参数见表 1。

表 1 探头参数
Table 1 Parameter of probe

频率 f/MHz	焦距 s/mm	晶片直径 d/mm	曲率半径 R/mm
10	38	12.7	17.15

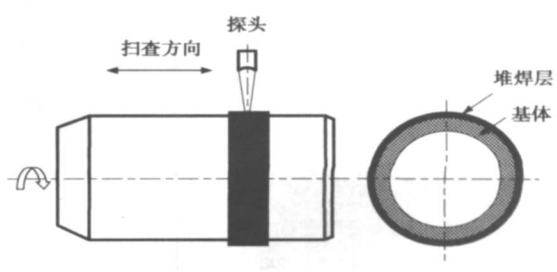

图 1 堆焊结构检测示意图
Fig. 1 Schematic of Inspection for surfacing weld

1.2 检测方法

试验采用超声C扫描成像的方法进行检测。C扫描成像是超声无损检测中发展较早，并且广泛应用的成像技术。检测中常以水为耦合介质，用聚焦探头以特定的扫描方式对垂直于声束方向的被测试样进行逐点扫描，记录每一点的反射回波信号，并且对其渡越时间信号进行采样和模数转换，运用现代信号和图像处理技术在计算机屏幕上直观地显示含有缺陷形状、位置及大小等信息的灰度或伪彩色图像，从而达到评价焊接质量的目的。

1.3 检测方案

从堆焊结构上看，超声入射方式有两种选择，从工件外部或者内部入射。从工件外部（铜侧）入射较方便，但要对堆焊层表面加工处理，否则粗糙的表面将使大部分超声波发生散射，难以保证超声波有足够的能量检测微小缺陷，导致检测灵敏度降低。若从工件内部（钢侧）入射，则不必对堆焊层表面加工处理，减少了机加工作量，但增加了检测难度。

2 聚焦超声垂直入射曲面工件内声场特性分析

试件表面形状对声束聚焦影响较大，聚焦探头发射的声束垂直入射到平板试件内部时，试件表面各个方向对声束的折射作用相同，若试件表面为柱面，其表面各个方向对声束的折射作用将发生变化。为了简化声场分析的复杂性，文中仅分析探头在两个互相垂直的平面内的声束传播“行为”。如图2所示，选取沿柱面轴线（A平面）与圆周（B平面）两个互相垂直的方向进行分析[8]。

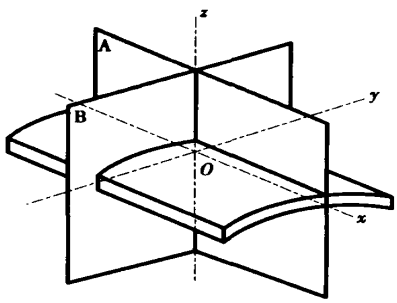

图2 沿圆柱轴线与圆周方向两个互相垂直平面

Fig. 2 Two planes of axial and radial to cylinder

研究中被测试件的堆焊层厚度为3 mm，基体直径为155 mm，经计算在A，B平面内的声学参数见表2。根据以上参数将声束垂直进入曲面试件内传播情况进行简单描述（图3），其中两个圆柱体近似表示声束在A，B两个互相垂直的平面内形成的聚焦区。由表2可知A，B平面内焦点深度差为0.27 mm，焦点直径相差0.04 mm，两焦柱重叠部分长度为1.59 mm。由以上参数分析可知，焦点直径相差很小，而且两焦柱重叠部分占整个焦柱长度的80%以上，通过调节耦合水层的距离，使两焦柱的重叠部分位于堆焊界面即可获得良好的检测效果。采用上述方法对声束从试件内部（钢侧）入射的传播情况做了同样的分析，与声束从外部入射的聚焦情况相似，在声束传播的两个互相垂直的平面内，焦点直径相差较小，聚焦区域仍有大部分的重叠，适当调整耦合水层距离，同样可以获得良好的检测效果，在此不做详细分析。

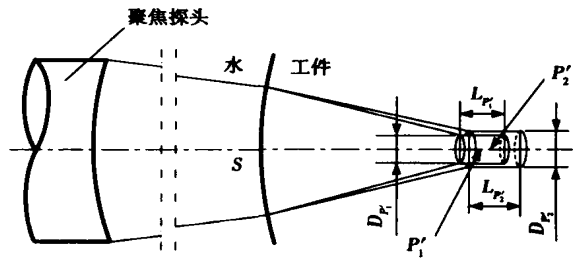

A 平面内：焦点深度 SP'_1；焦点直径 $D_{p'_1}$；焦柱长度 $L_{p'_1}$；焦点 P'_1

B 平面内：焦点深度 SP'_2；焦点直径 $D_{p'_2}$；焦柱长度 $L_{p'_2}$；焦点 P'_2

图3 声束在A和B平面内的传播示意图

Fig. 3 Schematic drawing of sound beam in plane A and B

表2 A和B平面内的声学参数

Table 2 Acoustic parameter of plane A and B

	焦点深度 h/mm	焦点直径 D/mm	焦柱长度 L/mm
A 平面内	3.00	0.44	1.70
B 平面内	3.27	0.48	2.02

综上所述，由于文中被测试件基体直径相对较大，试件表面形状对声束的折射作用影响较小，为了简化试验条件，采用平板代替圆柱形试件进行试验分析。

3 超声C扫描检测试验及结果分析

3.1 对比试件的制做及检测

为了获取合适的检测参数，根据被检测工件中缺陷的形貌特点，制做了带有模拟缺陷（人工反射体）的对比试件。在堆焊界面处常产生未熔合等面状缺陷，采用平底孔模拟此类缺陷，在堆焊试件上分

别从铜钢两侧加工了ϕ2 mm的平底孔。堆焊界面处的未熔合缺陷中存在空气隙，为空气—金属界面，而将平底通孔置于水中，为水—金属界面，与实际情况不符，为了模拟真实缺陷，要将平底通孔进行密封处理，这样一方面更接近真实缺陷，另一方面也降低了制做对比试件的复杂性。图 4a 为其中从铜侧入射检测的对比试件，反复调整检测参数得到对比试件的最佳检测工艺，超声检测结果见图 4b。

3.2　堆焊试件的检测及分析

利用上述试验获取的检测工艺分别从铜钢两侧入射检测了堆焊试件，检测结果见图 5。为了验证检测结果的可靠性，分别对图 5b 中的四个典型位置进行了破坏性检测，图 6 为破坏性检测结果。

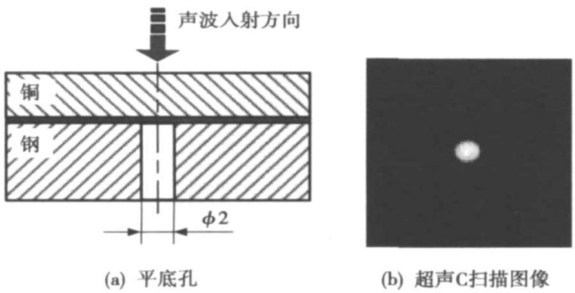

图 4　对比试件的超声 C 扫描检测

Fig. 4　C-scan image of reference test piece

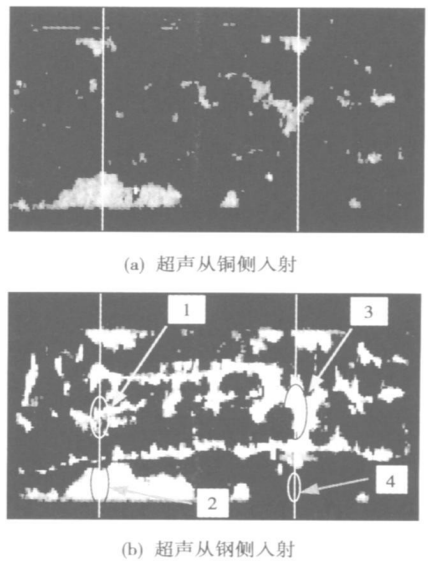

图 5　堆焊试件的超声 C 扫描检测结果

Fig. 5　C-scan image of surfacing piece

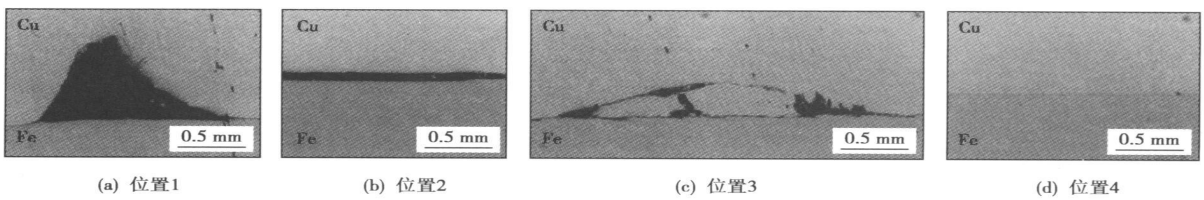

图 6　破坏性检测

Fig. 6　Destructive test

对比图 5a 和图 5b 超声 C 扫描图像，同时结合图 7 相应位置的界面反射 A 扫描波形（实线为超声从铜侧入射，点划线为从钢侧入射）发现，在位置 1 处声波从铜表面入射时界面反射波幅值较低；而从钢表面入射时界面反射波幅值较高，与ϕ2 mm 平底孔的反射波幅值相当，由此可判断该处存在焊接缺陷。从图 6 中的金相照片可以看出，缺陷断面近似呈三角形，尖端深入到堆焊层内部，由缺陷的形貌特征可知，超声波从铜侧入射时缺陷尖端对声波产生散射作用，使反射波幅值降低。在位置 2 处声波从铜、钢两侧入射界面反射波幅值均比较高，根据超声信号可判断该处有缺陷。从金相照片上看，该处是大面积的未熔合缺陷。位置 3 处声波从铜、钢两侧入射检测结果一致，与破坏性检测结果吻合，该处也存在大面积的缺陷。位置 4 处界面反射波幅值非常低，应为结合良好的界面，由于两种材料声阻抗的差异，超声波在完全结合的界面处仍有部分发生反射。

结合超声 C 扫描检测图像及相应的 A 扫描信号，并和破坏性检测结果对比发现，声波从铜侧入射检测结果的可靠性明显低于从钢侧入射，大部分缺陷被漏检。因此应根据缺陷的形貌特征制订合理的检测工艺，对于文中试验的检测对象，采用从钢侧入射的检测方式，能够提高缺陷的检出率，对堆焊结构做出合理的质量评价。

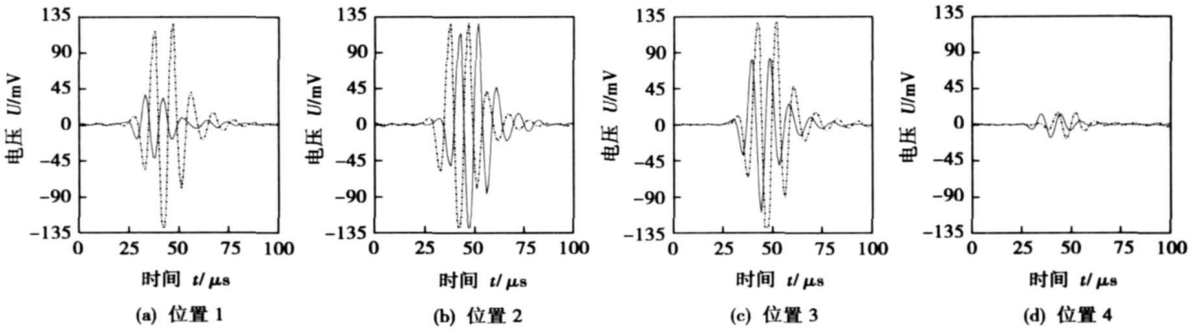

图 7 界面反射信号

Fig. 7 Reflective signal on interface

4 结 论

(1) 超声 C 扫描成像检测方法能够有效完成铜钢堆焊接头的质量评价, 可靠性较高。

(2) 试件表面形状对声束传播有一定影响。聚焦探头发射的声束垂直入射到圆柱形试件内部, 当圆柱直径较大时, 圆柱面对声束聚焦的影响可以忽略。

(3) 对于堆焊接头, 在条件允许的情况下, 应采用从基体一侧入射方式进行检测, 以获得较高的可靠性。

参考文献:

[1] 吕念春, 牛济泰, 国旭明, 等. 紫铜与不锈钢的焊接[J]. 材料科学与工艺, 2000, 8 (2): 46—50.

[2] 何 鹏, 冯吉才, 钱乙余, 等. 接触反应法解决铝/不锈钢钎焊的缺陷及脆性[J]. 材料科学与工艺, 2005, 13 (1): 82—85.

[3] 宋敏霞, 赵熹华, 郭 伟, 等. 钛合金与其它金属材料扩散连接研究现状与发展[J]. 焊接, 2005(1): 5—7.

[4] 王克鸿, 徐越兰, 王建平, 等. 弹带熔敷扩散焊接技术研究[J]. 兵器材料科学与工程, 2002, 25 (2): 34—36.

[5] 王克鸿, 徐越兰, 余 进, 等. 无槽弹带焊接技术研究[J]. 弹道学报, 2001, 13 (3): 47—51.

[6] Ciocan R, Soare M, Revenco V. Quality evaluation of the end-plate welds and brazed joints for CANDU nuclear fuel by an ultrasonic imaging method [J]. Insight: Non-Destructive Testing and Condition Monitoring, 1997, 39 (9): 622—625.

[7] Kwon S D, Choi M S, Lee S H. The applications of ultrasonic backward radiation from a layered substrate submerged in liquid [J]. NDT&E International, 2000, 33 (5): 275—281.

[8] 张志永. 水浸聚焦超声波探伤原理[M]. 北京: 国防工业出版社, 1985.

作者简介: 高双胜, 男, 1974 年出生, 博士研究生。主要从事超声无损检测与评价方面的研究。发表论文 6 篇。

Email: gaoshsh@hit.edu.cn

fracture on the 1Cr17Ni2 side was cleavage and quasi-cleavage mixture, which confirmed that the HAZ of 1Cr17Ni2 base metal was the weakest area in the joint to result in the crack and leakage. The other failure reasons were also analyzed and the measures were put forward to solve the problem.

Key words: stainless steel; tungsten inert-gas welding joint; failure analysis

Numerical analysis of electron beam welding and local heat treatment combination technology HU Meijuan, LIU Jinhe (School of Materials Science and Engineering, Northwestern Polytechnical University, Xi'an 710072, China). p93—96, 100

Abstract: Electron beam welding and local heat treatment is a new combination processing technology. Its temperature and stress fields were computed by finite element method with ANSYS software code, and 2 mm, 6 mm and 12 mm thick TC4 titanium alloy plates were taken as the researched objects. The influence rules of local heat treatment on temperature and stress fields of electron beam welding for different thickness plates were analyzed. It is found that the effect of electron beam local heat treatment of 2 mm thick titanium alloy plate is the best under the given computational condition. Within the distance of 4 mm from the centerline at the surface, cooling rate are almost the same after electron beam local heat treatment. The maximum longitudinal residual stress reduces from 780 MPa to 560 MPa. The decrease amplitude reaches 28%.

Key words: electron beam welding; titanium alloy; local heat treatment; numerical simulation

Laser welding technology and properties of macromolecule material plastics XIE Long, LIU Liming (State Key Laboratory of Materials Modification, Dalian University of Technology, Dalian 116024, Liaoning, China). p97—100

Abstract: Based on the theory of laser welding of plastic, the polypropylene plate was welded by laser welding, and the feasibility of laser welding of thermoplasties was ivestigated. The weld appearance showed the weld is approaching to the base metal in color. After the welding line being brittlly failed with liquid nitrogen, silver was sprayed on the fracture surface. Then the fracture surface was analyzed by scanning electron microscope, and flashes or impurities were not observed. Mechanical properties of the welded joint were tested. The mechanical properties of the polypropylene joint with laser welding was approaching to that of the base mental. It proves that laser welding is not only a feasible, but also a perfect plastics welding method.

Key words: welding; laser; plastics; fracture appearance; mechanical properties

Ultrasonic signal character and quality evaluation of Cu/steel surfacing weld GAO Shuangsheng[1], GANG Tie[1], GUI Guangzheng[2], YUAN Yuan[1] (1. State Key Laboratory of Advanced Welding Production Technology, Harbin Institute of Technology, Harbin 150001, China; 2. Baoshan Iron & Steel Co. Ltd, Shanghai 201900, China). p101—104

Abstract: By using water immersion focusing method in an ultrasonic C-scan inspection system, the quality of Cu/steel surfacing weld was evaluated. The sound field in the two planes of axial and radial to the cylinder were analyzed when the sound beam vertically incidents into the cylindrical work piece. Based on the above theoretical analyses, surfacing welds were inspected by C-scan mode. In order to verify the reliability of ultrasonic test, ultrasonic A-scan signals received from typical area of the workpiece were studied and the corresponding destructive test was done. The result shows that it is feasible to evaluate the surfacing weld by using the proposed method. Moreover, the tested result is more reliable when sound beam incidents into the piece from the base metal.

Key words: dissimilar material joining; surfacing; ultrasonic C-scan; water immersion focusing

Interfacial reaction of Sn-9Zn/Cu joint with Cu particle-reinforced composite solder Sn-9Zn WEI Guoqiang[1], KUANG Min[2], YANG Yongqiang[1] (1. School of Mechanical Engineering, South China University of Technology, Guangzhou 510640, China; 2. Materials Surface Centre, Guangzhou Research Institute of Nonferrous Metals, Guangzhou 510651, China). p105—108

Abstract: The influences of Cu-particle addition in Sn-9Zn lead-free solder powder (composite solder) on the interfacial reaction of Sn-9Zn/Cu joint were investigated under extended reflowing time conditions. The results show that Cu-particle addition in Sn-9Zn lead-free solder decreases dramatically the growing rate of the interfacial intermetallic compound (IMC) in Sn-9Zn/Cu joint, consequently which results in the reduction of the interfacial IMC layers and Kirkendall defect in the interfacial IMC layers. The thickness of IMC layers increases with increasing reflowing time and decreases with increasing Cu-particle content in Sn-9Zn lead-free solder. EDX analysis of IMC layer indicates that it is only composed of Cu—Zn intermetallic compounds there is no Cu—Sn intermetallic compounds to befound under existing test conditions.

Key words: lead-free solder; composite solder; Sn—9Zn solder; interfacial reaction; microstructure

Three dimensional numerical simulation for explosive welding WANG Jianmin, ZHU Xi, LIU Runquan (Department of Naval Architecture & Ocean Engineering, Naval University of Engineering, Wuhan 430033, China). p109—112

Abstract: Explosive welding process was numerically simulated with 3D by nonlinear finite element software MSC. Dytran. Velocity and pressure distribution were also calculated during explosive welding process. The numerically simulated results were compared with theoreticaly calculated results, which showed that the numerically simulated results were much similar with theoretic results. The results indicates that the mathematical model can be exactly to simulate explosive welding. Velocity and pressure distribution during explosive welding process can be simulated simply by Dytran. However, it can't simulate the formation of jet and wave-form in explosive welding. The simulation can be referred to explosive welding technology.

Key words: explosive welding; numerical simulation; pressure; velocity